

# Geometry-Independent Hypersonic Boundary-Layer Transition Prediction

*Daniel B. Araya, Neal P. Bitter, and Hicham Alkandry*

## ABSTRACT

*One of the fundamental challenges of fielding and maneuvering a hypersonic vehicle is predicting the large changes in heat transfer and aerodynamic performance associated with the transition of the surface boundary-layer flow from laminar to turbulent during flight. Legacy methods for analyzing boundary-layer transition are overly simplistic and do not account for the intricate flow patterns of modern vehicles with complex three-dimensional shapes. This article introduces work utilizing a novel methodology, known as input/output (I/O) analysis, recently applied to hypersonic flows. This methodology is completely free of geometric constraints and has significant potential to answer many of the open questions in transition analysis. The article presents examples of I/O analysis applied to hypersonic flow over a 7° half-angle sharp cone and to the Boundary Layer Transition (BOLT) flight experiment. The analysis uses computational tools that were built in collaboration with the University of Minnesota and VirtusAero as part of a Johns Hopkins University Applied Physics Laboratory (APL) independent research and development project.*

## INTRODUCTION

A well-known phenomenon in fluid physics is the existence of a thin region of flow near the surface of an object in motion, called a boundary layer, which is characterized as either laminar, turbulent, or transitional depending on conditions. The boundary-layer flow can have a dramatic impact on the forces and heat transferred to a vehicle during flight, and thus predicting when it transitions from laminar to turbulent has been the subject of intense academic research over many decades.<sup>1-4</sup> A visualization of the different boundary-layer states over a sharp cone in free flight is shown in Figure 1. The imaging technique highlights strong density gradients in the flow, including across shocks and within the bound-

ary layer. The left inset in Figure 1 shows the flow near the nose of the cone, where the boundary-layer flow is smooth and laminar. Far downstream (right inset), the boundary-layer flow has transitioned to a turbulent state, characterized by chaotic, small-scale fluctuations that are captured in the density contours of the image.

The impact of boundary-layer transition on vehicle performance varies with speed, but a significant effect observed across all speed regimes is an increase in drag with turbulent flow. This happens because a turbulent boundary layer always has a steeper velocity gradient at the wall, independent of speed, which is directly proportional to the skin friction drag. For hypersonic flows, total



**Figure 1.** Shadowgraph image of boundary-layer transition. This image is over a 5° half-angle sharp cone traveling at Mach = 4.31 in free flight at an aeroballistics range. Labels of boundary-layer states and cropped image insets have been added. (Adapted from Schneider,<sup>5</sup> with permission from Elsevier.)

drag can increase by up to 70% with transition to turbulent flow for conical bodies,<sup>6</sup> which becomes a design challenge when vehicle range or other constraints sensitive to drag are a priority. Aside from a drag penalty, a major detrimental effect of transition for hypersonic flow is a large rise in surface heating. Hypersonic turbulent heat transfer rates can exceed five times laminar values,<sup>7</sup> and transitional heating “overshoot” is a known phenomenon that even further exceeds these levels.<sup>8</sup> From a practical standpoint, the overall increase in surface heating posed by hypersonic transition necessitates an increase in thermal protection for a vehicle, which adds weight and further constrains its range and maneuverability. Other aspects of hypersonic transition that are less widely studied but still important to vehicle performance include the effects of transition on aerodynamic control effectiveness<sup>9,10</sup> and aero-optics for vehicle sensing.<sup>11</sup>

It is clear that capturing transition effects is important to balance robust design with optimal performance for hypersonic vehicles. Despite this knowledge, a fundamental challenge for vehicle designers today is that legacy methods to predict transition are overly simplistic and cannot account for the highly three-dimensional flow patterns of complex shapes, leading to significant errors and often overconservatism in design. Two examples that highlight the highly three-dimensional flows for non-axisymmetric geometries are shown in Figure 2. The images are from computational fluid dynamics (CFD) simulations for hypersonic flow over a generic finned cone<sup>12</sup> and for the Boundary Layer Tran-

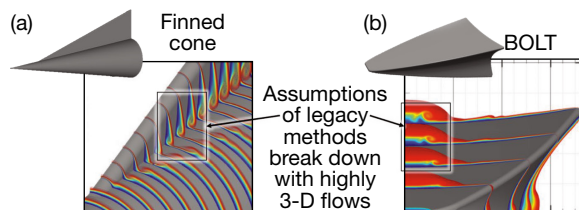


**Figure 2.** CFD examples. Shown are highly three-dimensional flows for (a) the finned cone (from Mullen et al.,<sup>12</sup> with permission) and (b) the BOLT geometry (from Thome et al.,<sup>13</sup> reprinted by permission of the American Institute of Aeronautics and Astronautics, Inc.)

sition (BOLT) flight experiment.<sup>13,14</sup> (See the article by Wheaton, in this issue, for more on BOLT.) The colors in the figure represent streamwise velocity contours at different axial stations along each body. The large swirling patterns that emerge near the fin-cone intersection and in the middle of the concave surface of BOLT are clear indications of strong gradients in the flow, which can cause legacy transition prediction methods to fail for reasons explained in the next section.

Ultimately, the shortcomings of transition predictions translate into uncertainties in aerothermal and aerodynamic predictions that a vehicle designer must manage with appropriate design margins. Such uncertainties may be compounded over long trajectories deep within the atmosphere, where the effects of transition and turbulence can dominate, thus driving a critical need for improved modeling of the transition process. This article describes the implementation and early results of a novel transition prediction technique known as input/output (I/O) analysis done in collaboration with the University of Minnesota and VirtusAero. The I/O method stems from linear systems theory and is based on resolvent analysis with a long mathematical history that has only very recently been applied to hypersonic boundary-layer flows.<sup>15</sup> Critically, the I/O method is independent of assumptions about the structure of the flow field considered and thus has the potential to answer a number of fundamental questions in boundary-layer stability and transition that could lead to unique hypersonic vehicle designs.

## TRANSITION PREDICTION METHODS

Despite more than 60 years of study, boundary-layer transition is still not completely understood and the development of theoretical models remains an important and active area of research.<sup>4</sup> The physics of the transition process is a complex initial-boundary value problem where flow perturbations enter a laminar boundary layer and, if unstable, are amplified by a variety of mechanisms until the amplitude of the perturbations is sufficiently large to induce nonlinear breakdown to turbulence. A simplistic representation of this process is shown in Figure 3<sup>16</sup> for flow over a flat plate with the boundary-layer height,  $\delta$ , exaggerated for illustration. In the sketch, the disturbance within the boundary layer is represented by a wavy line that grows in amplitude downstream until eventually morphing into a more chaotic pattern, indicative of turbulence.

Transition onset is known to be extremely sensitive to initial and boundary conditions and is a significant contributor to large aerothermal modeling uncertainty.<sup>5</sup> The state of the practice for predicting transition onset for vehicle design purposes is to use simplistic correlations based on historical flight test data from sphere-cone geometries.<sup>17</sup> Although these correlations are

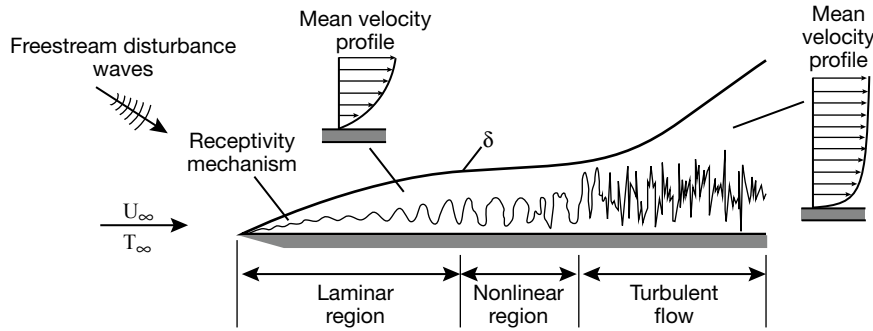


**Figure 3.** Simplified schematic of disturbance growth and boundary-layer transition for flow over a flat plate. The disturbance within the boundary layer is represented by a wavy line that grows in amplitude downstream until eventually morphing into a more chaotic pattern, indicative of turbulence. (Reprinted with permission from Avallone.<sup>16</sup>)

sometimes useful, they lack any underlying physical model of the flow and thus also lack general predictive power. Physics-based transition prediction methods such as linear stability theory (LST) and parabolized stability equations (PSE) have been used for several decades to examine the linear growth of modal disturbances to a laminar boundary layer such as Mack’s second-mode and stationary crossflow waves.<sup>4</sup> Numerical LST/PSE solvers can now be used routinely to determine the growth of modal (wave-like) disturbances and arrive at predictions of a transition N-factor, where N is a quantitative measure of the exponential growth of the amplitude of an initial disturbance. The larger the N-factor, the greater the exponential growth of the disturbance, and typically a threshold value (e.g.,  $N = 5$ ) is used to estimate the onset of boundary-layer transition along the surface of a body. At a high level, the underlying assumptions of LST and PSE limit their application to relatively simple geometric configurations, where it can be assumed that the flow changes gradually except in just one direction and that flow disturbances travel along prescribed paths. These assumptions break down when considering highly three-dimensional flows, so the methods must be used with caution when trying to predict transition along vehicles with complex geometric features, such as near control surfaces.

Over the last decade, several novel high-fidelity tools for predicting transition on complex shapes have been developed. These include BiGlobal stability analysis,<sup>18,19</sup> plane-marching PSE,<sup>20,21</sup> nonlinear PSE,<sup>22</sup> linearized direct numerical simulation (DNS),<sup>23,24</sup> and resolvent-based I/O analysis.<sup>15,25,26</sup> Of these methods, I/O and linearized DNS are the least restrictive in their assumptions about the underlying base flow; however, both still require some choice to be made about how the laminar flow is perturbed in the simulation. One example would be to introduce small-amplitude acoustic waves of a specific frequency at the far-field boundary. This choice can affect the results, since transition mechanisms are

necessary temporal and spatial scales to carry the simulation all the way through breakdown to turbulence, which has been done successfully for simple axisymmetric cases.<sup>27</sup> However, such an approach is extremely computationally expensive, even for simple geometries, and is therefore impractical for engineering analysis of transition over more complex shapes and flight-like conditions.

To give context to the aforementioned transition prediction methods, Figure 4 presents an adaptation

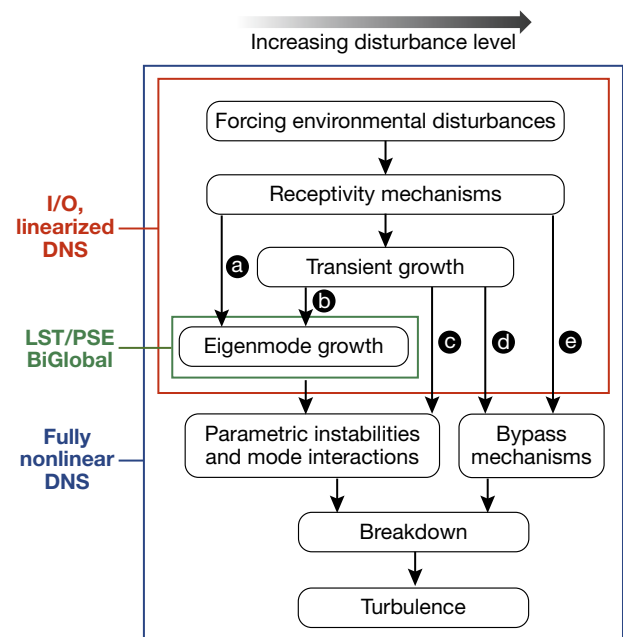


**Figure 4.** Morkovin transition diagram. This diagram illustrates how the transition process is understood as progressing along pathways, each of which depends on various parameters of the mean flow and disturbances. The colored boxes have been added to show how the transition prediction methods can be categorized according to levels of modeling fidelity, with the I/O method covering all possible linear pathways (a–e) up to nonlinear breakdown. (Adapted from Fedorov.<sup>4</sup>)

of a diagram widely reproduced in the boundary-layer transition community and known as the Morkovin transition diagram. This diagram illustrates how the transition process is understood as progressing along different pathways that are each dependent on numerous parameters of the mean flow and disturbances. The colored boxes have been added to show how the transition prediction methods can be categorized according to levels of modeling fidelity, with the I/O method covering all possible linear pathways (a–e) up to nonlinear breakdown.

## I/O THEORY

As with all linear stability analysis methods, I/O attempts to answer the basic question of whether a small disturbance to an equilibrium state will either attenuate or grow in such a way that the system cannot return to its original state. For boundary-layer transition analysis, the I/O system in question is the fluid flow, which is governed by the compressible Navier–Stokes equations, expressed in a compact form as follows:

$$\frac{\partial U}{\partial t} = F(U).$$

Here the vector  $U = [\rho, \rho u, \rho v, \rho w, E]$  represents conserved fluid variables—namely the density and three components of linear momentum and energy, respectively. The right-hand side defines a nonlinear function of the fluid fluxes for each of the conserved variables that describes the transport of mass, momentum, and energy throughout the fluid and also introduces temperature and pressure through the energy equation. These equations can be closed according to the properties of the fluid being considered. For a perfect gas,  $p = \rho RT$  is used to relate pressure ( $p$ ), density ( $\rho$ ), and temperature ( $T$ ) with a specific gas constant,  $R$ .

The equilibrium fluid state is known as the base flow, which is a steady-state laminar flow solution to the Navier–Stokes equations. As the name implies, linear stability analysis involves examining the linear response of perturbations to a given base flow. This can be represented as  $U = \bar{U} + U'$ , where  $\bar{U}$  represents the base flow solution and  $U'$ , the flow perturbations. Substituting this summation into the nonlinear fluid equations and neglecting all but terms that are linear in  $U'$  results in the linearized Navier–Stokes equations. After discretizing, the linearized equations can be expressed as

$$\frac{\partial U_i'}{\partial t} = A_{ij} U_j'.$$

Here the index  $i$  refers to the  $i$ th degree of freedom. For example, a two-dimensional problem with  $N_x$  and  $N_y$  computational cells in the  $x$ - and  $y$ -directions (respectively) and four governing equations ( $\rho, u, v, T$ ) has  $N = 4 \times N_x \times N_y$  total degrees of freedom, so index  $i = [1, N]$ . We also introduced the Jacobian matrix,  $A_{ij}$ ,

which represents the linearized dynamics of the perturbations about the base flow and is calculated from the nonlinear function of the fluid fluxes as

$$A_{ij} = \frac{\partial \mathcal{F}_i(U_1, U_2, \dots, U_N)}{\partial U_j},$$

where, more generally,  $N = N_{eq} \times N_{cells}$ ,  $N_{eq}$  is the number of equations,  $N_{cells}$  is the number of grid cells, and  $\mathcal{F}_i$  is the discretized Navier–Stokes operator corresponding to the  $i$ th degree of freedom. The I/O method incorporates forcing into the fluid system through additions to the linearized equations,

$$\frac{\partial U_i'}{\partial t} = A_{ij} U_j' + B_{ij} f_j$$

$$y_i = C_{ij} U_j',$$

where the input forcing,  $f$ , is defined within the domain through the matrix  $B$ , and the fluid response,  $y$ , is measured within the domain through the matrix  $C$ . The choice of the input forcing and where to apply it in the domain is left to the analyst to decide, as described in the previous section. Analytically, the solution to this linear system can be obtained by taking a Fourier transform of the equations and solving algebraically to give

$$\hat{y}_i = C_{ij} (-i\omega I_{ij} - A_{ij})^{-1} B_{ij} \hat{f}_j,$$

where the term  $(-i\omega I_{ij} - A_{ij})^{-1}$  is known as the resolvent matrix, and  $\omega$  is the temporal frequency of the input forcing under consideration (i.e.,  $f = \hat{f} e^{-i\omega t}$ ). Computing the resolvent matrix is the key step in the I/O analysis that determines the flow response to a given perturbation. This resolvent can be solved in a number of ways, but typically the problem is formulated as an optimization problem, where the response obtained is the result of maximizing some quantity (e.g., disturbance energy) for a given input.

Once the I/O response has been calculated, the spatial growth of the perturbation can be obtained from its amplitude, and estimates of boundary-layer transition can be made based on the conventional N-factor method or some other criterion such as correlations of breakdown amplitude. For simple systems (e.g., those with only a few hundred degrees of freedom), the resolvent matrix can easily be computed by directly inverting  $(-i\omega I_{ij} - A_{ij})$ . For three-dimensional fluid systems, however, there can be millions of degrees of freedom, creating a very large and sparsely populated Jacobian matrix. Solving this linear system then quickly becomes the bottleneck to utilizing the I/O method efficiently for complex flow problems. Despite this challenge, the potential of the I/O method has been demonstrated for fully three-dimensional and PSE-based implementations of boundary-layer transition,<sup>28,29</sup> and efforts are underway to explore iterative matrix methods for solving more complicated flow problems.<sup>26</sup>

## US3D IMPLEMENTATION

To obtain the necessary base flows for transition analysis, we utilize the CFD software US3D,<sup>30</sup> which has been used for a number of programs across APL over the years. The code was originally developed at the University of Minnesota in the early 2000s and is now commercially licensed and maintained through VirtusAero. US3D is well known for its accurate simulations of thermochemical nonequilibrium gas flows, particularly for hypersonics. As an integral part of an APL independent research and development project to investigate I/O, we collaborated with the US3D developers at the University of Minnesota and VirtusAero in an effort to build and test a series of US3D software add-ons, called plug-ins, to implement the I/O method. This effort intentionally focused on using the existing US3D software infrastructure rather than building a new code, a strategy that was intended to minimize development time and ensure portability of the new I/O capability.

The general steps in the I/O boundary-layer transition analysis workflow and its US3D implementation are as follows:

- **Step 1: Given a geometry and flow conditions, compute a high-fidelity, steady laminar solution to the Navier–Stokes equations (i.e., the base flow).** This step can be executed using the US3D software as is. Of critical importance to I/O is obtaining a base flow with sufficiently small grid spacing to enable resolution of boundary-layer instabilities along any of the spatial directions of interest. Achieving this grid spacing typically requires a much higher streamwise density of grid points than other stability analysis methods requires. A good rule of thumb is to include at least 10 grid cells per wavelength of the instability of interest.
- **Step 2: Determine the linearized dynamics of small fluctuations about the computed base flow, represented by a Jacobian matrix,  $A_{ij}$ .** For this step, a new US3D plug-in was developed by our collaborators to numerically compute the Jacobian using the fluxes already computed by the finite-volume solver within US3D. In addition, a quad-precision build of US3D was required for the current I/O implementation because of the relatively small value of the perturbed quantities and the fact that US3D uses dimensional variables.
- **Step 3: Define a linear system with user-defined forcing at input locations in the computational domain, as well as in output locations to measure the flow response.** For this step, a second plug-in was developed by VirtusAero to allow users to selectively “tag” grid cells within the fluid domain, both for defining input forcing and output response locations. This plug-in was built outside of the main solver as part of the US3D post-processor tools.
- **Step 4: Solve the I/O linear system to determine the flow response to forcing (i.e., the spatial growth or decay of initial perturbations over a range of temporal frequencies).** Again using the US3D post-processor framework, a third plug-in was developed by our collaborators for this final step in the I/O analysis. As an initial approach, the software package MUMPS<sup>31</sup> was built in to a new version of US3D to allow for a parallelized “direct” solution of the sparse linear algebra system. Direct methods compute the inverse of a matrix by directly factoring the matrix (e.g., by lower-upper decomposition). Such an approach becomes limited by computer memory for very large matrices but has been demonstrated to work well for simple two-dimensional fluid problems.<sup>25</sup>
- **Step 5: Make a transition prediction based on an accepted boundary-layer transition criterion.** This final step in the workflow is not specific to I/O or dependent on US3D but is rather a choice for the analyst. One of the most attractive features of I/O is the potential to solve the so-called receptivity problem, where freestream disturbances are tracked through a shock and transition can be predicted with knowing the initial disturbance amplitudes and having an amplitude-based transition criterion (see, e.g., Marineau et al.<sup>32</sup>). Otherwise, the conventional N-factor–based method can also be done with I/O by using, for example, amplification of pressure fluctuations at the wall.

The remainder of this article steps through two hypersonic flow examples that use the new US3D I/O infrastructure to examine boundary-layer instabilities. Because the US3D I/O development work is ongoing, we present only preliminary results that focus on steps 1–4 in the I/O transition prediction procedure, along with a summary and discussion of future work.

## SHARP CONE

The first test of the new US3D I/O code focused on a comparison with published experimental data for a well-known boundary-layer instability for hypersonic flows—namely, Mack’s second-mode instability. Specifically, we considered measurements of the amplitude of second-mode waves for the flow over a 7° half-angle sharp cone conducted at the Arnold Engineering Development Complex (AEDC) Hypervelocity Wind Tunnel 9 facility.<sup>33</sup> The base flow for the test case was computed using the conditions provided for Tunnel 9 experimental run 3745. The sharp cone considered was aligned with the freestream, and the incoming flow was at Mach = 9.39 and unit Reynolds number of  $Re = 1.81 \times 10^6/m$ .

Figure 5 shows Mach contours for the sharp cone base flow computed with US3D for the Tunnel 9 conditions.

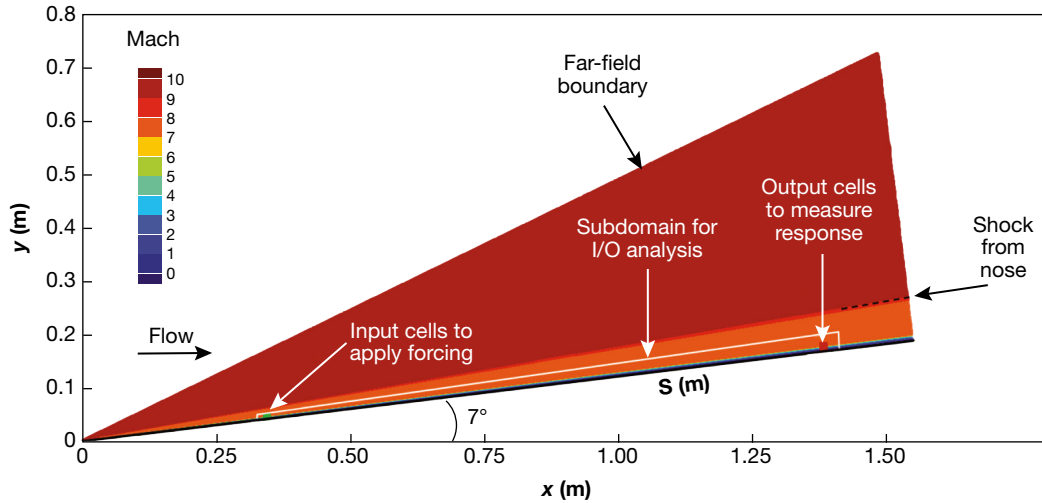


**Figure 5.** Laminar base flow solution for I/O analysis of the sharp cone. Flow conditions correspond to Tunnel 9 run 3745 experimental conditions; Mach = 9.39,  $Re = 1.81 \times 10^6/m$ .

To simplify the computation, the flow is assumed to be axisymmetric, as intended in the experiment. In reality, the computational domain is a three-dimensional wedge with symmetry boundary conditions in the azimuthal directions. Rather than executing the I/O analysis on the entire flow field, the analysis is performed in a smaller region (a subdomain) of the flow where the instability is active. The main shock from the nose of the cone as well as the I/O subdomain and input and output cells selected for analysis are labeled in the figure. It is important to note that the size of the I/O subdomain and input and output cells within it can be selected arbitrarily and is guided by the experiment in this case. Constraining the I/O subdomain to beneath the shock avoids potential numerical issues with accurately resolv-

ing the instability relative to the shock. The results' sensitivity to the choice of subdomain and input and output cell locations remains an open question for future study.

For reference, the base flow shown in Figure 5 includes 6,025 grid points in the streamwise direction and 200 grid points in the wall-normal direction. For this simple case, even though the base flow could be obtained with far fewer grid points in the streamwise direction, a coarser mesh was not able to properly resolve the streamwise flow instability. According to the Tunnel 9 experiment, the frequency of the dominant second-mode instability along the sharp cone was 78 kHz for run 3745 flow conditions. The streamwise wavelength of the second-mode instability can be estimated as  $\lambda \approx 0.9U/f$ , where  $U$  is the freestream

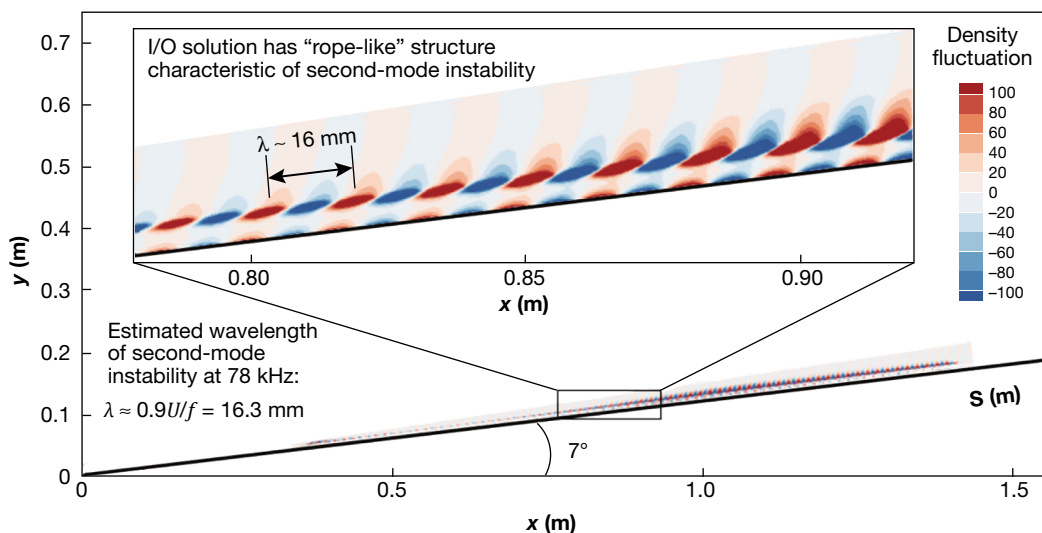


**Figure 6.** Result of I/O analysis for the sharp cone subject to 78 kHz upstream forcing. Colors correspond to density fluctuations of the dominant I/O response.

velocity and  $f$  is the frequency of the instability. Thus, the minimum streamwise grid spacing in this case is  $\Delta s \approx 0.1\lambda \approx 1.6$  mm. Upon refinement, we found that a grid spacing of roughly half this estimate, or  $\Delta s \approx 0.07$  mm, did best to resolve the second-mode instability, which is visualized by contours of density fluctuations ( $\rho'$ ) in Figure 6. This contour plot represents the solution to the I/O analysis (i.e., the dominant response of the flow to upstream forcing at a frequency of 78 kHz).

The rope-like structure of the density fluctuations shown in Figure 6 is a typical characteristic of the second-mode instability, which is formed by packets of planar waves that grow in the streamwise direction within the boundary layer. Upon further inspection, we found that the wavelength of the observed density fluctuations is  $\lambda \approx 16$  mm, which closely corresponds to the initial estimate of the second-mode wavelength of  $\lambda \approx 16.3$  mm. Finally, once the spatial growth of the dominant instability has been calculated, a boundary-layer transition prediction can be made. In this case, the experiments used high-frequency pressure transducers to directly measure the amplitude of the second-mode wave as it passed over the cone surface. The onset of boundary-layer transition was observed in the experiment to occur between  $S = 1.0$  and  $1.2$  m with a maximum N-factor of  $N_{max} = 3.5$ . An analogous analysis of second-mode growth can be estimated from the I/O response by extracting the growth of the density fluctuations at the wall, shown in Figure 7. The maximum N-factor can be estimated by computing the natural log of the ratio of the maximum to minimum peak amplitude of the density fluctuation at the wall. This was calculated as  $N_{max} \approx 2.93$  at  $S = 1.01$  m, in reasonable agreement with the experiment.

## BOLT

While the sharp cone test case validates the new US3D I/O code capability, there are simpler and well-established means of predicting the amplitude growth of the second-mode instability for the hypersonic flow over a cone. The LST method is one example, although I/O can produce additional rich spatial information about the instability that LST could not. The true power of the I/O method, however, is that, in principle, it can be applied to arbitrarily complex three-dimensional flows in the same way that it is applied to simpler two-dimensional ones. Much less is known about boundary-layer instabilities for such complex flows, so there is potentially a great deal of insight to gain from I/O analysis.

To highlight a stressing multidimensional test case for the new US3D I/O code, we examined the flow field for the BOLT geometry referenced in the introduction. The I/O analysis procedure for BOLT matched the procedure for the cone exactly, with the first step being to compute a highly resolved laminar base flow. An example of this base flow computed with 163 million grid cells is shown in Figure 8. The view in the figure is from the front, and only one quarter of the flow field is analyzed because of its symmetry. Surface heating is shown in gray scale, and axial slices of streamwise velocity are shown in the color contours. The flow conditions correspond to a point during the ascent phase of the planned BOLT flight—namely, Mach = 5 and  $Re = 5 \times 10^6/m$ . As mentioned before, properly resolving the laminar base flow is critical to accurately capturing the growth of instabilities. For BOLT, it turns out that resolving all these laminar features is quite challenging to compute, especially near the centerline where large vortical structures emerge within a thick boundary layer. More details on the laminar base flow computations for BOLT and the associ-

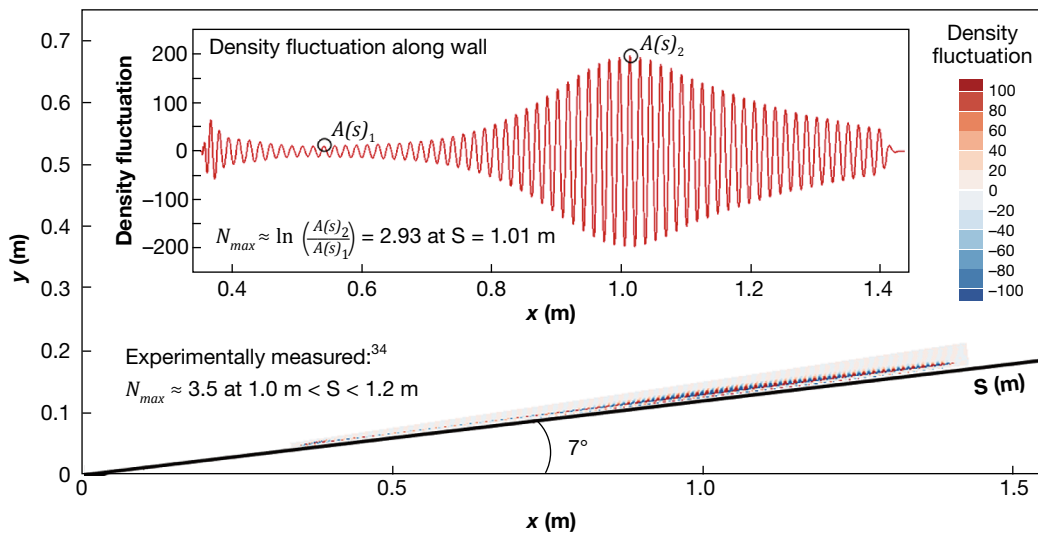


**Figure 7.** Result of I/O analysis for sharp cone subject to 78 kHz upstream forcing. Inset shows extraction of density fluctuation along the wall for estimating maximum N-factor for second-mode instability.

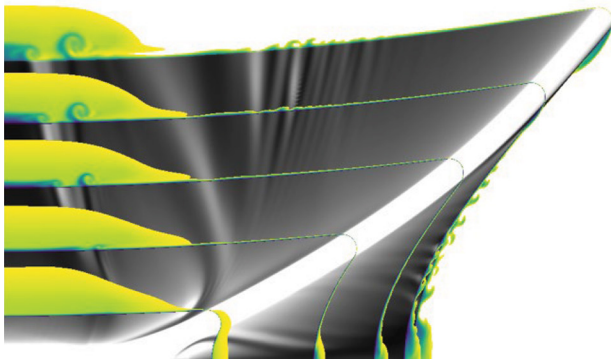


**Figure 8.** Laminar base flow computation for BOLT. The solution includes 163 million grid points. Color contours are axial slices of streamwise velocity, and surface heat flux is shown in gray scale. (Courtesy of John Thome at the University of Minnesota.)

ated nuances with the numerical algorithms employed are provided in Thome, Knutson, and Candler.<sup>34</sup> What is important to highlight here is that streamwise vortices are thought to play an important role in the evolution of boundary-layer instabilities. The large vortical structures near the centerline of BOLT could serve as one of the pathways to transition, but such a hypothesis cannot be tested using legacy stability analysis methods alone.

For flows that vary significantly in just two directions, the BiGlobal linear stability analysis method is applicable. When coupled with a planar PSE marching technique, BiGlobal has been successfully used to examine streamwise vortical instabilities for hypersonic vehicles such as BOLT.<sup>35</sup> Details of the BiGlobal method are beyond the scope of this article, but we note that APL has recently added BiGlobal with PSE marching as another tool for boundary-layer transition analysis through a code development partnership with Sandia National Laboratories. Using this BiGlobal code, we targeted a small subdomain of the centerline flow field for BOLT to produce a base-line solution for comparison with I/O. It is important to emphasize that there is no technical reason for BiGlobal and I/O to produce exactly the same result, since fundamentally BiGlobal is constrained to a planar eigenmode analysis and I/O is more generalized. Still, the slow change in the flow field in the streamwise direction for BOLT suggests that there is good reason to trust that BiGlobal would correctly identify the dominant centerline instabilities and thus is a good measure for comparison with I/O.

The main result of the BiGlobal analysis is the prediction of a dominant vortex instability situated atop one of the centerline streamwise vortices for BOLT. This instability occurs at a frequency of 100 kHz and has a streamwise wavelength of 15 mm. A three-dimensional reconstruction of this vortical instability is presented in Figure 9 alongside the result from the US3D I/O analysis for the same disturbance frequency. These early results are believed to be the first application of the I/O method to three-dimensional hypersonic flows with a direct comparison to the BiGlobal with PSE marching method. Axial slices of the mean streamwise velocity are shown in the figure by green and purple contours, and iso-contours of density fluctuations are shown in red and blue. In both cases, the density fluctuation exhibits a clear wave-like pattern that steadily grows in amplitude as it travels downstream. The I/O result appears to be significantly under-resolved, with many small-scale features apparent in the density contours that are probably numerical artifacts. Still, when compared to the BiGlobal result, it is significant that I/O predicts the presence of an instability above the same centerline vortex and with roughly the same streamwise wavelength. We anticipate that closer agreement with BiGlobal could be achieved with finer grid refinement for the I/O analysis in this case.

It should also be noted that the rectangular subdomain shown in Figure 9 was purposefully constrained to a small region of the flow with just  $120 \times 50 \times 50$  grid points. Limiting the size of this three-dimensional subdomain was necessary to capture the instability using the US3D I/O code in its current form. In actuality, BiGlobal analysis was executed first over a much larger subdomain, and these results were used to identify the vortical instability and target appropriate domain

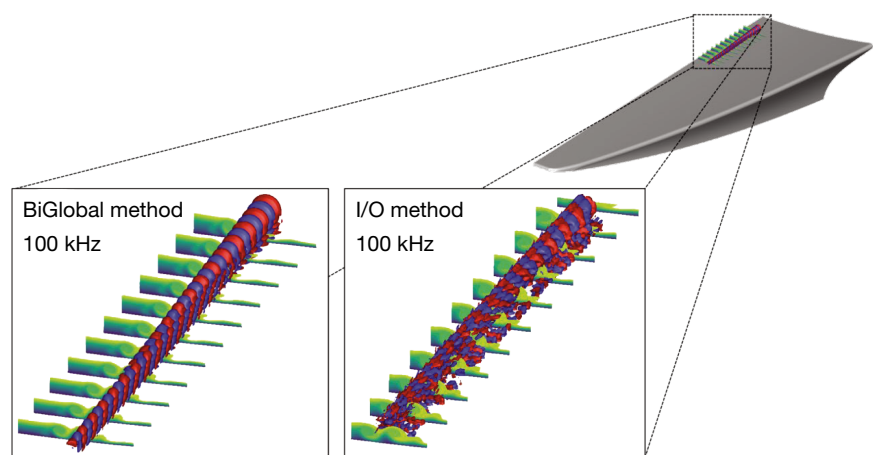


**Figure 9.** Qualitative comparison of BiGlobal and I/O analysis predictions of centerline vortical instability for BOLT during ascent. Base flow Mach = 5 and  $Re = 5 \times 10^6/m$ . Green and purple contours correspond to axial slices of streamwise velocity. Red and blue iso-contours correspond to three-dimensional reconstruction of density fluctuations for the dominant instability.

extents and grid spacing requirements for the I/O analysis. Ideally, the restriction on domain size for the I/O analysis could be lifted and the method applied to the entire flow field at once. This seems achievable but will require further study on efficiently computing the resolvent, which is the true bottleneck for the I/O method today. Computing the resolvent is a known technical, not physical, limitation of I/O; surmounting this challenge could unlock the method's full potential for predicting boundary-layer transition for arbitrarily complex hypersonic flows.

## SUMMARY AND FUTURE WORK

Two main takeaways from this work are that it resulted in (1) demonstration of I/O analysis capability built in to a commercial CFD code that has powerful potential to predict hypersonic boundary-layer instabilities independent of geometric configuration, and (2) a successful collaboration with university and industry leaders to transfer high-impact technology from academia to the application space through APL.

During this project, new software plug-ins were developed and shared by collaborators at the University of Minnesota and VirtusAero to incorporate the I/O analysis procedure into the existing framework of the well-established US3D code. Two hypersonic test cases were evaluated with the newly developed US3D I/O code, including flow over a 7° half-angle sharp cone and the BOLT geometry. I/O predictions for the second-mode instability for the sharp cone were consistent with published experimental data from AEDC Tunnel 9 experiments and highlighted the method's strict grid spacing requirements. We found that streamwise spacing of approximately 5% of the second-mode wavelength was best able to resolve the instability for the cases attempted. For the three-dimensional BOLT flow field, BiGlobal analysis with planar PSE marching was applied first and identified a dominant vortex instability near the centerline. We used this result to define a smaller subdomain for the US3D I/O analysis, which ultimately produced results that qualitatively agree with the BiGlobal predictions. Further refinement of the I/O results using the direct matrix method we used requires significant computer memory, and the inclusion of an iterative solver with the US3D I/O code is critical to apply the method to practical three-dimensional problems.

We are continuing this work as part of a new APL project sponsored by the Office of Naval Research under Dr. Eric Marineau. As part of this 3-year effort, APL will continue its collaboration with the University of Minnesota and VirtusAero to further develop and test the US3D I/O code for complex geometries relevant to the Navy and more broadly to the Department of Defense.

**ACKNOWLEDGMENTS:** This work was partially funded by the Force Projection Sector Precision Strike Mission Area (PSMA) as part of an independent research and development project for fiscal year 2020. We thank PSMA executive Kirk Shawhan, PSMA chief scientist Glenn Mitzel, and former group chief scientist Dr. Sarah Popkin for their guidance and support. In addition, the work would not have been possible without the significant contributions from Dr. Heath Johnson of VirtusAero and Professor Joseph Nichols of the University of Minnesota. We are also grateful to University of Minnesota Professor Graham Candler and all of his and Professor Nichols's students who shared their US3D experience and insight with us, especially John Thome and Anthony Knutson for sharing their computational grids and high-resolution base flow computations.

The views, opinions, and/or findings expressed are those of the authors and should not be interpreted as representing the official views or policies of the Department of Defense or the US government.

## REFERENCES

- <sup>1</sup>W. S. Saric, H. L. Reed, and E. J. Kerschen, "Boundary-layer receptivity to freestream disturbances," *Annu. Rev. Fluid Mech.*, vol. 34, pp. 291–319, 2002, <https://doi.org/10.1146/annurev.fluid.34.082701.161921>.
- <sup>2</sup>W. S. Saric, H. L. Reed, and E. B. White, "Stability and transition of three-dimensional boundary layers," *Annu. Rev. Fluid Mech.*, vol. 35, pp. 413–440, 2003, <https://doi.org/10.1146/annurev.fluid.35.101101.161045>.
- <sup>3</sup>Y. S. Kachanov, "Physical mechanisms of laminar-boundary-layer transition," *Annu. Rev. Fluid Mech.*, vol. 26, pp. 411–482, 1994, <https://doi.org/10.1146/annurev.fl.26.010194.002211>.
- <sup>4</sup>A. Fedorov, "Transition and stability of high-speed boundary layers," *Annu. Rev. Fluid Mech.*, vol. 43, pp. 79–95, 2011, <https://doi.org/10.1146/annurev-fluid-122109-160750>.
- <sup>5</sup>S. P. Schneider, "Hypersonic laminar–turbulent transition on circular cones and scramjet forebodies," *Prog. Aerosp. Sci.*, vol. 40, no. 1–2, pp. 1–50, 2004, <https://doi.org/10.1016/j.paerosci.2003.11.001>.
- <sup>6</sup>C. P. Knisely, C. H. Haley, and X. Zhong, "Impact of hypersonic boundary layer transition on skin drag and surface heating on blunt cones," in *Proc. AIAA Scitech 2019 Forum*, AIAA 2019-1134, <https://doi.org/10.2514/6.2019-1134>.
- <sup>7</sup>M. S. Holden, T. P. Wadhams, M. MacLean, and E. Mundy, "Review of studies of boundary layer transition in hypersonic flows over axisymmetric and elliptic cones conducted in the CUBRC shock tunnels," in *Proc. 47th AIAA Aerospace Sci. Mtg.*, 2009, AIAA-2009-782, <https://doi.org/10.2514/6.2009-782>.
- <sup>8</sup>K. J. Franko and S. K. Lele, "Breakdown mechanisms and heat transfer overshoot in hypersonic zero pressure gradient boundary layers," *J. Fluid Mech.*, vol. 730, pp. 491–532, 2013, <https://doi.org/10.1017/jfm.2013.350>.
- <sup>9</sup>M. J. Terceros and D. Araya, "Influence of boundary layer transition on the aerodynamics of a sliced cone with ramp at Mach 6," in *Proc. AIAA Scitech 2021 Forum*, AIAA 2021-1852, <https://doi.org/10.2514/6.2021-1852>.
- <sup>10</sup>J. Tan, J. Tu, X. Sun, F. Liu, L. Meng, and P. Yang, "Numerical study of hypersonic shock-wave/laminar boundary-layer interactions of a typical lifting vehicle," in *Proc. 21st AIAA Int. Space Planes and Hypersonics Tech. Conf.*, 2017, AIAA 2017-2280, <https://doi.org/10.2514/6.2017-2280>.
- <sup>11</sup>S. Lee, M. C. Jeong, I. S. Jeung, H. J. Lee, and J. K. Lee, "Aero-optical measurement in shock wave of hypersonic flow field," in *Proc. 30th Int. Symp. Shock Waves I*, 2017, pp. 229–232.
- <sup>12</sup>C. D. Mullen, A. Moyes, T. S. Kocian, and H. L. Reed, "Parametric boundary-layer stability analysis on a hypersonic finned circular cone," in *Proc. 2018 Fluid Dyn. Conf.*, AIAA 2018-3072, <https://doi.org/10.2514/6.2018-3072>.

- <sup>13</sup>J. Thome, A. Dwivedi, J. W. Nichols, and G. V. Candler, "Direct numerical simulation of BOLT hypersonic flight vehicle," in *Proc. 2018 Fluid Dyn. Conf.*, AIAA 2018-2894, <https://doi.org/10.2514/6.2018-2894>.
- <sup>14</sup>B. M. Wheaton, D. C. Berridge, T. D. Wolf, D. B. Araya, R. T. Stevens, et al., "Final design of the Boundary Layer Transition (BOLT) flight experiment," *J. Spacecraft Rockets*, vol. 58, no. 1, pp. 6–17, 2021, <https://doi.org/10.2514/1.A34809>.
- <sup>15</sup>J. W. Nichols and G. V. Candler, "Input-output analysis of complex hypersonic boundary layers," in *Proc. AIAA Scitech 2019 Forum*, AIAA 2019-1383, <https://doi.org/10.2514/6.2019-1383>.
- <sup>16</sup>F. Avallone, "Application of non-intrusive experimental techniques to roughness-induced transition in hypersonic flows," PhD dissertation, Delft University of Technology, Delft, Netherlands, 2015.
- <sup>17</sup>K. F. Stetson, "Comments on hypersonic boundary-layer transition," Wright Research and Development Center, Wright-Patterson AFB, Dayton, Ohio, Tech. Rep. 90-3057, 1990, <https://apps.dtic.mil/sti/citations/ADA227242>.
- <sup>18</sup>P. Paredes, M. Hermanns, S. Le Clainche, and V. Theofilis, "Order  $10^4$  speedup in global linear instability analysis using matrix formation," *Comp. Methods App. Mech. Eng.*, vol. 253, pp. 287–304, 2013, <https://doi.org/10.1016/j.cma.2012.09.014>.
- <sup>19</sup>P. Paredes and V. Theofilis, "Spatial linear global instability analysis of the HIFiRE-5 elliptic cone model flow," in *Proc. 43rd AIAA Fluid Dyn. Conf.*, 2013, AIAA 2013-2880, <https://doi.org/10.2514/6.2013-2880>.
- <sup>20</sup>P. Paredes, V. Theofilis, D. Rodriguez, and J. Tendro, "The PSE-3D instability analysis methodology for flows depending strongly on two and weakly on the third spatial dimension," in *Proc. 6th AIAA Theor. Fluid Mech. Conf.*, 2011, AIAA-2011-3752, <https://doi.org/10.2514/6.2011-3752>.
- <sup>21</sup>P. Paredes, A. Hanifi, V. Theofilis, and D. Henningson, "The nonlinear PSE-3D concept for transition prediction in flows with a single slowly-varying spatial direction," *Procedia IUTAM*, vol. 14, pp. 36–44, 2015, <https://doi.org/10.1016/j.piutam.2015.03.021>.
- <sup>22</sup>C.-L. Chang, "The Langley Stability and Transition Analysis Codes (LASTRAC): LST, linear & nonlinear PSE for 2D, axisymmetric, and infinite swept wing boundary layers," in *Proc. 41st Aerosp. Sci. Mtg. Exhib.*, 2003, AIAA-2003-974, <https://doi.org/10.2514/6.2003-974>.
- <sup>23</sup>O. Browne, A. Haas, H. Fasel, and C. Brehm, "An efficient strategy for computing wave-packets in high-speed boundary layers," in *Proc. 47th AIAA Fluid Dyn. Conf.*, 2017, AIAA-2017-3636, <https://doi.org/10.2514/6.2017-3636>.
- <sup>24</sup>A. P. Haas, O. M. F. Browne, H. F. Fasel, and C. Brehm, "A time-spectral approximate Jacobian based linearized compressible Navier-Stokes solver for high-speed boundary-layer receptivity and stability," *J. Comput. Phys.*, vol. 405, article 108978, 2020, <https://doi.org/10.1016/j.jcp.2019.108978>.
- <sup>25</sup>D. A. Cook, J. Thome, J. M. Brock, J. W. Nichols, and G. V. Candler, "Understanding effects of nose-cone bluntness on hypersonic boundary layer transition using input-output analysis," in *Proc. 2018 AIAA Aerosp. Sci. Mtg.*, AIAA-2018-0378, <https://doi.org/10.2514/6.2018-0378>.
- <sup>26</sup>D. A. Cook, A. Knutson, J. W. Nichols, and G. V. Candler, "Matrix methods for input-output analysis of 2D and 3D hypersonic flows," in *Proc. AIAA Scitech 2020 Forum*, AIAA-2020-1820, <https://doi.org/10.2514/6.2020-1820>.
- <sup>27</sup>C. Hader and H. F. Fasel, "Towards simulating natural transition in hypersonic boundary layers via random inflow disturbances," *J. Fluid Mech.*, vol. 847, R3, 2018, <https://doi.org/10.1017/jfm.2018.386>.
- <sup>28</sup>D. Tempelmann, A. Hanifi, and D. S. Henningson, "Spatial optimal growth in three-dimensional boundary layers," *J. Fluid Mech.*, vol. 646, pp. 5–37, 2010, <https://doi.org/10.1017/S0022112009993260>.
- <sup>29</sup>D. Tempelmann, A. Hanifi, and D. S. Henningson, "Spatial optimal growth in three-dimensional compressible boundary layers," *J. Fluid Mech.*, vol. 704, pp. 251–279, 2012, <https://doi.org/10.1017/jfm.2012.235>.
- <sup>30</sup>G. V. Candler, H. B. Johnson, I. Nompelis, V. M. Gidzak, P. K. Subbareddy, et al., "Development of the US3D code for advanced compressible and reacting flow simulations," in *Proc. 53rd AIAA Aerosp. Sci. Mtg.*, 2015, AIAA-2015-1893, <https://doi.org/10.2514/6.2015-1893>.
- <sup>31</sup>P. R. Amestoy, I. S. Duff, J. Y. L'Excellent, and J. Koster, "MUMPS: A general purpose distributed memory sparse solver," in *Applied Parallel Computing. New Paradigms for HPC in Industry and Academia. PARA 2000. Lecture Notes in Computer Science*, vol. 1947, T. Sørsvik, F. Manne, A. H. Gebremedhin, and R. Moe, Eds., 2000, pp. 121–130, [https://doi.org/10.1007/3-540-70734-4\\_16](https://doi.org/10.1007/3-540-70734-4_16).
- <sup>32</sup>E. C. Marineau, G. Grossir, A. Wagner, M. Leinemann, R. Radespiel, et al., "Compilation and analysis of second-mode amplitudes on sharp cones in hypersonic wind tunnels," in *Proc. 2018 AIAA Aerosp. Sci. Mtg.*, AIAA 2018-0349, <https://doi.org/10.2514/6.2018-0349>.
- <sup>33</sup>E. C. Marineau, G. C. Moraru, D. R. Lewis, J. D. Norris, J. F. Lafferty, et al., "Mach 10 boundary layer transition experiments on sharp and blunted cones," in *Proc. 19th AIAA Int. Space Planes Hypersonic Syst. Technol. Conf.*, 2014, AIAA-2014-3108, <https://doi.org/10.2514/6.2014-3108>.
- <sup>34</sup>J. Thome, A. Knutson, and G. V. Candler, "Boundary layer instabilities on BoLT subscale geometry," in *Proc. AIAA Scitech 2019 Forum*, 2019, AIAA 2019-0092, <https://doi.org/10.2514/6.2019-0092>.
- <sup>35</sup>M. M. Choudhari, F. Li, and P. Paredes, "A computational analysis of boundary layer instability over the BOLT configuration," in *Proc. AIAA Scitech 2021 Forum*, AIAA-2021-1207, <https://doi.org/10.2514/6.2021-1207>.



**Daniel B. Araya**, Force Projection Sector, Johns Hopkins University Applied Physics Laboratory, Laurel, MD

Daniel B. Araya is a project manager in APL's Force Projection Sector. He earned an MS in aerospace engineering from Texas A&M University and an MS and a PhD in aeronautics from the California

Institute of Technology. Daniel's doctoral work focused on the dynamics of wake vortices in full-scale and laboratory-scale experiments of vertical-axis turbines. Over the last decade, he has obtained experimental and computational experience across a wide array of problems in fluid physics, ranging from high-Reynolds-number subsonic free-shear flows, high-energy plasma jets, and most recently hypersonic boundary-layer flows. He is currently a co-principal investigator (co-PI) for the Boundary Layer Transition (BOLT) post-flight research and BOLT II flight test support project sponsored by the Air Force Office of Scientific Research, a key collaborator on a Depart-

ment of Defense High Performance Computing Modernization Program Frontier project to study turbulence at hypervelocity flight conditions, and the PI on an Office of Naval Research-sponsored project to study hypersonic transition and turbulence on complex geometries. He was an assistant professor of mechanical engineering at the University of Houston from 2016 to 2018, is a senior member of AIAA, and is a member of the AIAA Fluid Dynamics Technical Committee. His email address is [daniel.araya@jhuapl.edu](mailto:daniel.araya@jhuapl.edu).



**Neal P. Bitter**, Force Projection Sector, Johns Hopkins University Applied Physics Laboratory, Laurel, MD

Neal P. Bitter is an aerospace engineer in APL's Force Projection Sector. He earned a BS in mechanical engineering from the Milwaukee School of Engineering and an MS and a PhD in aeronautics from the Cal-

ifornia Institute of Technology. Neal's doctoral work focused on computational analysis of the stability of hypervelocity boundary layers. While working at Sandia National Laboratories, he participated in numerous turbulence research projects, including a Department of Defense High Performance Computing Modernization Program Frontier (DOD HPCMP) project for which he executed large-scale direct numerical simulation (DNS) of high-Reynolds-number turbulent flow, including multiphysics effects, in support of the Navy railgun program. He also spent several years using Sandia's SPARC computational fluid dynamics (CFD) code, working with large Department of Energy computing platforms to perform DNS involving billions of degrees of freedom and up to millions of CPU or GPU cores. In addition to this turbulence work, Neal has spent the majority of his career developing novel tools for predicting hypersonic boundary-layer transition. He has served as the principal investigator (PI) on several research and development projects in boundary-layer transition and turbulence. Currently he is the PI for a DOD HPCMP Frontier project focused on using DNS to better understand and model turbulence at hypervelocity flight conditions and co-PI on an Office of Naval Research-sponsored project to study hypersonic transition and turbulence on complex geometries. His email address is [neal.bitter@jhuapl.edu](mailto:neal.bitter@jhuapl.edu).



**Hicham Alkandry**, Air and Missile Defense Sector, Johns Hopkins University Applied Physics Laboratory, Laurel, MD

Hicham Alkandry is a member of APL's Senior Professional Staff in the Aerospace and Mechanical Engineering Group of APL's Air and Missile Defense Sector. He received a BS in aerospace engineering

from Syracuse University and an MS and a PhD in aerospace engineering and scientific computing from the University of Michigan. Before joining APL in 2016, Hicham was a postdoctoral fellow in the Nonequilibrium Gas and Plasma Dynamics Laboratory at the University of Michigan from 2012 to 2014 and a senior systems engineer at Raytheon Missile Systems from 2014 to 2016. His specialty is high-speed aero-thermodynamics and in particular computational fluid dynamics techniques for modeling hypersonic flows. He has contributed to several journal and conference papers and received the AIAA David Weaver Best Student Paper Award in 2012. He is a senior member of AIAA and a current member of the AIAA Hypersonic Technologies and Space Planes (HyTASP) Technical Committee. His email address is [hicham.alkandry@jhuapl.edu](mailto:hicham.alkandry@jhuapl.edu).